RESEARCH ARTICLE

https://doi.org/10.1007/s11467-023-1369-0

Room-temperature ferroelectricity in van der Waals SnP_2S_6

Chaowei He[1,*], Jiantian Zhang[1,*], Li Gong[2], Peng Yu[1,†]

[1]State Key Laboratory of Optoelectronic Materials and Technologies
Guangzhou Key Laboratory of Flexible Electronic Materials and Wearable Devices
Nanotechnology Research Center, School of Materials Science and Engineering
Sun Yat-sen University, Guangzhou 510275, China

[2]Instrumental Analysis and Research Center, Sun Yat-sen University, Guangzhou 510275, China

[*]These two authors contributed equally to this work.

Corresponding author. E-mail: [†]yupeng9@mail.sysu.edu.cn

Received September 27, 2023; accepted November 13, 2023

Supporting information

1. Structural characterization of SnP_2S_6

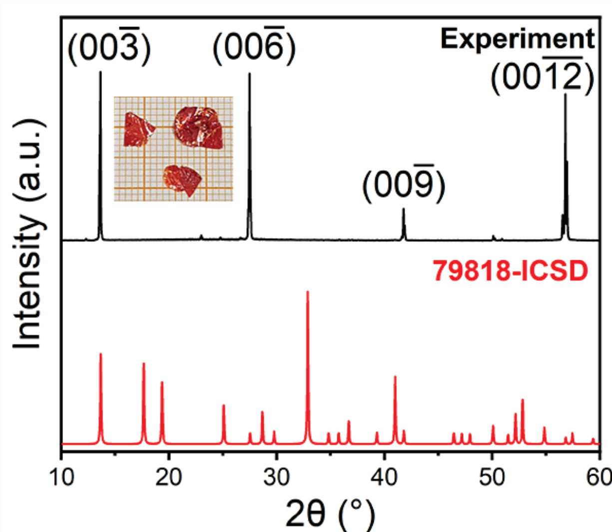

Fig. S1 XRD patterns of SnP_2S_6 single crystals.

The conventional wet-transfer method with the help of PMMA was used to transfer the exfoliated SnP_2S_6 flakes onto a Cu grid with a carbon film for preparation as a TEM sample. The atoms of the thin film exhibit uniform distribution, as shown in Fig. S2.

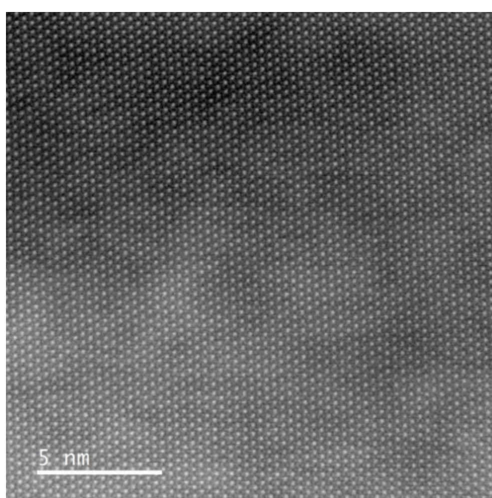

Fig. S2 STEM characterization of layered SnP_2S_6.

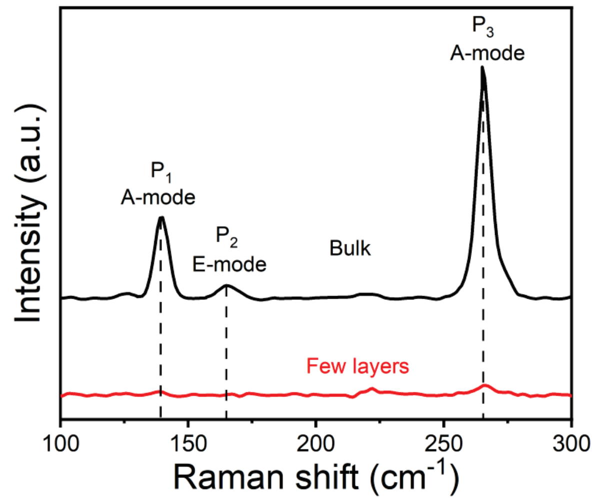

Fig. S3 Raman spectroscopy characterization of bulk and few-layer SnP_2S_6.

2. AFM and PFM characterization of SnP_2S_6 thin film

AFM can be used to analyze the surface morphology and film thickness of SnP_2S_6. Three flat surfaces of SnP_2S_6 thin films with different thicknesses were displayed (Fig. S4), and the amplitude and phase of PFM can detect point and dendritic undulations. Due to the exclusion of changes in the number of layers, it can be proven that there are ferroelectric domains with spontaneous polarization in the film. In the main text, the thin film that changes the polarization direction by applying voltage is 7nm, with a flat surface (Fig. S5).

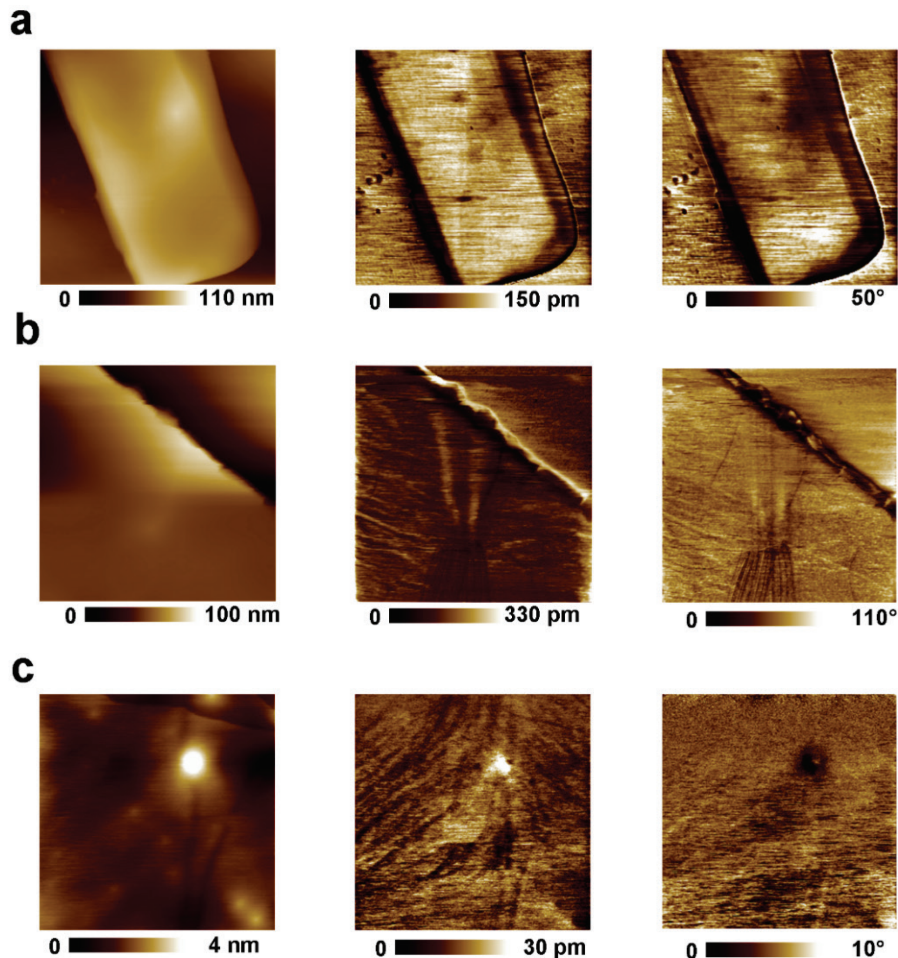

Fig. S4 AFM and piezoresponse images of SnP_2S_6 with different thickness.

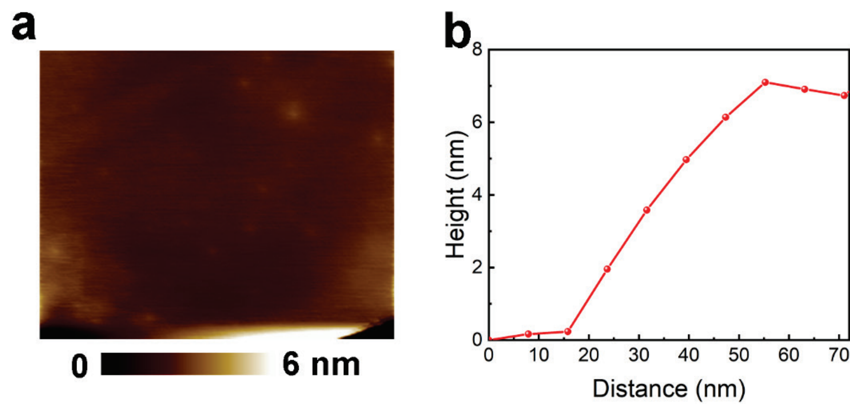

Fig. S5 AFM morphology **(a)** and thickness **(b)** of 7nm thin film with reverse DC bias box in box pattern.

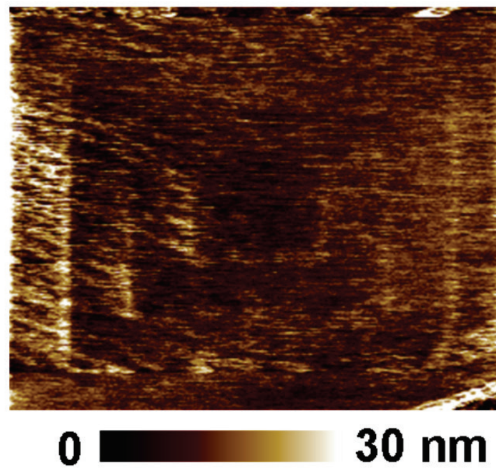

Fig. S6 PFM phase images of thin film for (g) with written box-in-box patterns at room temperature with reverse DC bias of +2 V, -2 V and +2 V.

3. Optoelelctronic characterization under lasers of different wavelengths

Comparisons were made on the photoresponse of multilayer graphene/SnP_2S_6/multilayer graphene heterostructure phototransistor under 405, 532, and 635 nm laser irradiation (Figs. S7 and S8). Under the same density, the photocurrent relationship generated by different wavelengths is 405 nm > 532 nm > 635 nm, while the response time is 405 nm < 532 nm < 635 nm. The result is suitable for both parallel and vertical heterojunctions. By comparing the parallel and vertical heterojunctions, it was found that the photocurrent and response speed of the vertical heterojunction were higher than those of the parallel heterojunction under three different wavelengths of irradiation.

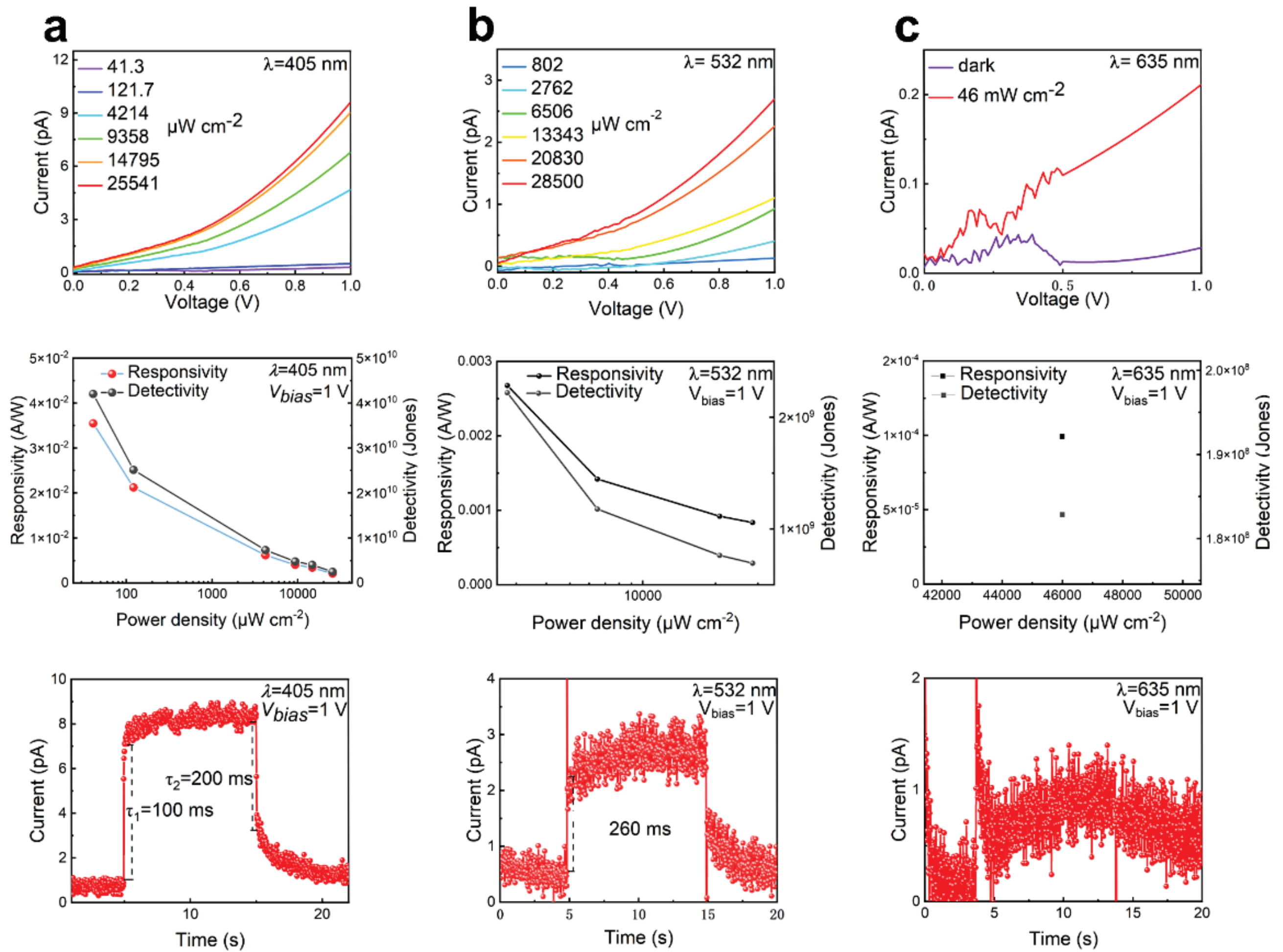

Fig. S7 Optoelectronic performance of SnP_2S_6 parallel photodetector at different wavelengths. **(a–c)** Output curves (top), responsivity and detectivity (middle), and photorespons time (bottom) of SnP_2S_6 parallel photodetector under 405 nm (a), 532 nm (b) and 635 nm (c) laser.

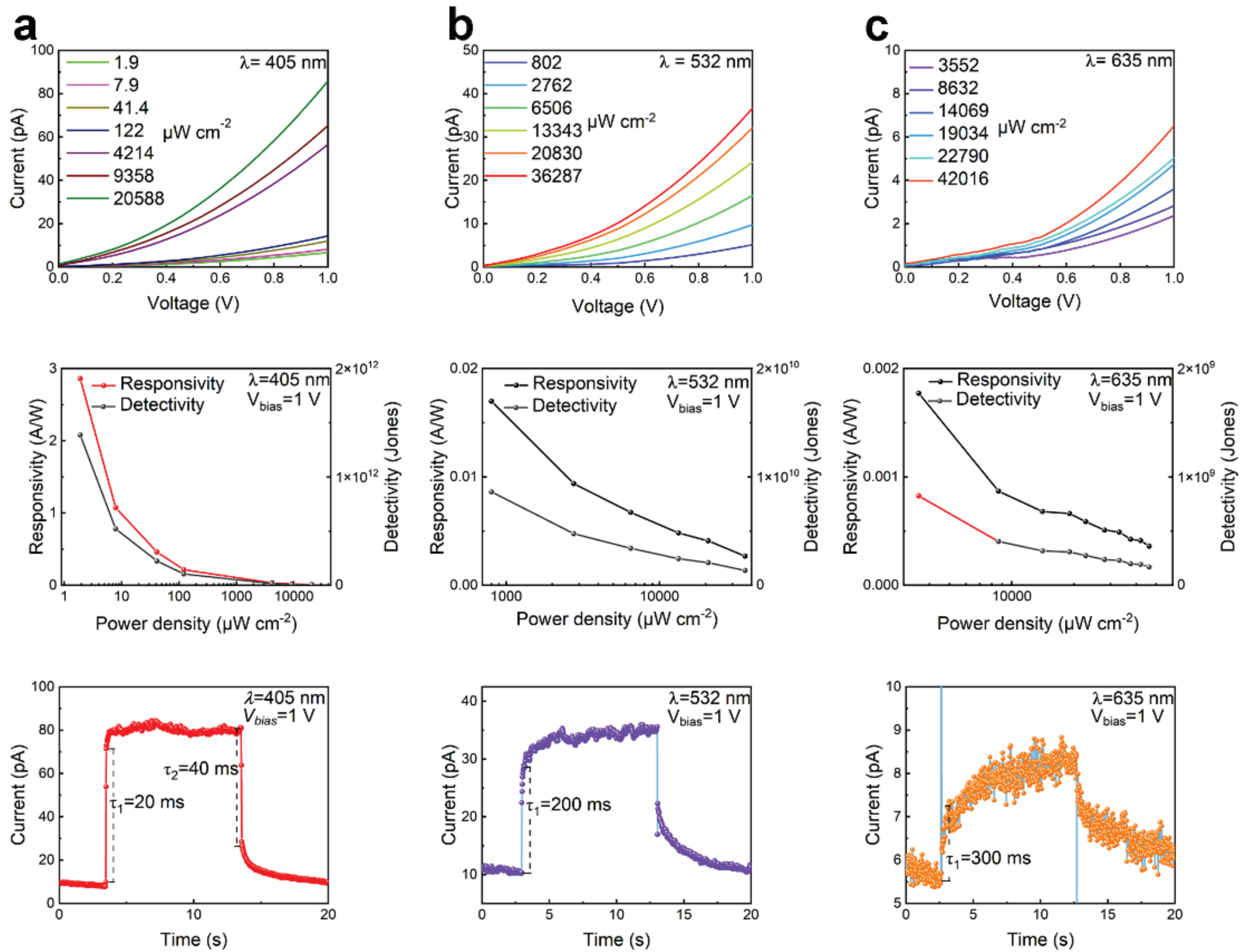

Fig. S8 Optoelectronic performance of SnP_2S_6 vertical transistors at different Wavelengths. **(a–c)** Output curves (top), responsivity and detectivity (middle), and photorespons time (bottom) of SnP_2S_6 vertical transistors under 405 nm (a), 532 nm (b) and 635 nm (c) laser.